SUPPLEMENTARY INFORMATION

An archaeal symbiont-host association from the deep terrestrial subsurface

Katrin Schwank[1], Till L. V. Bornemann[1], Nina Dombrowski[2], Anja Spang[2,3], Jillian F. Banfield[4] and Alexander J. Probst[1]*

[1] Group for Aquatic Microbial Ecology (GAME), Biofilm Center, Department of Chemistry, University of Duisburg-Essen, Germany
[2]Department of Marine Microbiology and Biogeochemistry (MMB), Royal Netherlands Institute for Sea Research (NIOZ), and Utrecht University, Den Burg, Netherlands
[3]Department of Cell- and Molecular Biology, Science for Life Laboratory, Uppsala University, SE-75123, Uppsala, Sweden
[4] Department for Earth and Planetary Sciences, University of California, Berkeley, USA

*to whom the correspondence should be addressed:
Alexander J. Probst
University of Duisburg-Essen
Universitätsstrasse 5
45141 Essen
alexander.probst@uni-due.de

Content:

1. Supplementary methods

Phylogenetic analysis

Hmm profiles of the 37 maker genes used by the phylosift v1.01 software [1, 2] were queried against a representative set of archaeal genomes from NCBI (182) and the GOLD database (3) as well as against the huberarchaeal population genome (for details on genomes please see Supplementary Data file 1) using the phylosift search mode [1, 2]. Protein sequences corresponding to each of the maker genes were subsequently aligned using mafft-linsi v7.407 [3] and trimmed with BMGE-1.12 (parameters: -t AA -m BLOSUM30 -h 0.55) [4]. All single protein alignments were subjected to phylogenetic analyses using IQ-tree v1.6.5 with the LG model and the tree topologies were visually inspected (iqtree -s alignment.phy -m LG -nt AUTO -bb 1000 -alrt 1000). This allowed us to select 34 proteins, in which major archaeal taxa formed monophyletic clusters suggesting that the corresponding genes were minimally affected by horizontal gene transfer. The 34 aligned and trimmed protein families were concatenated using catfasta2.phyml (https://github.com/nylander/catfasta2phyml) (alignment i) and recoded into four SR4 categories [5] (AGNPST = A, CHWY = T, DEKQR = C, FILMV = G) (alignment ii). Both alignments were subjected to maximum likelihood analyses as implemented by IQTREE (v1.6.5) under the mixture models LG+C60+F+R (alignment i, *Fig. 1A*) and the user defined C60SR4 model (alignment ii, Supplementary Data File 3) [6]. Support values were estimated using a SH-like approximate likelihood ratio test [7] and ultrafast bootstraps [8]. During the revision process the authors ran an updated phylogeny using all archaeal genomes available at NCBI (downloaded January 2019). Thereby, we recovered an additional genome of Huberarchaeota (ASM284167v1), which was included in *Fig. S1* to confirm the placement of the lineage within the phylogenetic analyses.

Furthermore, a smaller set of archaeal taxa was selected (which comprised in addition to Ca. *H. crystalense* 121 archaeal genomes from NCBI and two from the GOLD database) (Supplementary Data file 1) for Bayesian phylogenetic inferences based on the same set of 34 marker genes, which were aligned, concatenated and recoded as described above. Bayesian phylogenetic trees were inferred for the untreated and recoded alignment using the CAT-GTR model as implemented in PhyloBayes MPI v.1.7a [9]. For each alignment, a consensus tree was generated from two chains (sampling every fifth chain) once the maxdif had dropped below 0.15 (25% of the chains were discarded as burn-in).

NOTE: While the placement of Ca. *H. crystalense* within DPANN is supported in all analyses, the exact position of this genome relative to other DPANN clades needs to be further evaluated once additional genomes of members of this group are being available.

Pangenome analysis

For generating a comprehensive pangenome for detailed metabolic analyses, we used all available genomes from Ca. *Altiarchaeum hamiconexum* CG and Ca. *Huberiarchaeum chrystalense* [10]. This dataset encompassed at least ten individual genomes each, either from metagenomes or single-cell genomes [10]. We clustered [11] the predicted proteins of all genomes from metagenomes and single-cell genomes of either the host or the symbiont at 100% amino acid identity and selected the scaffolds of the centroids to define the pangenome. This was necessary as genomes of both the host and the symbiont were highly fragmented [10]. Some genetic redundancy in the pangenome, which stems from the fact that some scaffolds with centroids also carried non-centroid genes that had a 100% match in the dataset, did not interfere with the analysis. The data was uploaded and annotated via Genoscopes platform MAGE [12], at which the two pangenomes are publicly available as “Huberarchaea CG” and “Altiarchaeum CG”, respectively. Pathways were inferred using a combination of KEGG KOs [13] and final annotations from the MAGE platform. Some pathways were manually investigated and curated by inferring metabolic predictions for specific enzymes whose similarities are displayed in Supplementary Table 4 (manual annotation).

Co-occurrence analysis

To determine the co-occurrence analysis of Ca. *A. hamiconexum* CG and Ca. *H. crystalense* across 65 publicly available metagenome samples from Crystal Geyser [10, 14, 15], we mapped the quality filtered reads from these samples against the currently best genomes of the two organisms available from this ecosystem (quality was based on genome completeness, and N50). Reads were filtered for three mismatches (equals 98% error rate in a 150-bps read) and the coverage of each genome in each sample was determined using the iRep software [16]. Relative abundances were normalized based on the number of reads in each sample and analyzed using a Pearson correlation in the R software package [17].

Proportionality analysis. Relative genome abundances for a set of 505 dereplicated genomes [10] were determined by read mapping (Bowtie2 --sensitive [18]) followed by coverage calculation from reads that contained equal or less than three mismatches [16]. Only relative genomes were included if they had at least an average coverage of six in one of the samples (seven out of 505 genomes were excluded). The abundances were normalized using read counts ($\boldsymbol{Coverage} * \frac{\boldsymbol{max(read\ count)}}{\boldsymbol{read\ count}}$). The R [17] package propR [19] was used to analyze the proportionality [20] of the coverage profiles. Genome coverages were transformed using centered log-transformation and the False-Discovery-Rate was estimated to be 0% at a ρ cutoff of 0.70. To analyze only the most relevant co-occurrences, the minimal ρ was further increased to 0.90 and a network was generated and visualized using the R package iGraph [21]. Read-normalized abundances of organisms with a proportionality $\rho \geq 0.90$ with Ca. Altiarchaeum CG were visualized using Tableau 10.5.12.

Fluoresence in situ hybridization (FISH)

Groundwater fluids from the Crystal Geyser were filtered onto carbon coated 0.2-µm filters [especially designed for fluorescence microscopy (Millipore, Burlington, USA)] until the filters clogged (~60 ml). The samples were taken during the minor eruption phase of Crystal Geyser, during which the Altiarchaeota and Huberarchaeota abundance was the greatest [10]. Afterwards, the cells were fixed with 3% formaldehyde (16% formaldehyde (w/v) diluted in 1xPBS) for one hour at room temperature. Fixed cells were washed three times with 1xPBS. The fixed cells were stored at room temperature.

A specific probe for the 16S rRNA gene sequence of Ca. *H. crystalense* was designed using the ARB software package [22]. The probe was specific to the lineage due to the highly diverging 16S rRNA gene and did not match any other 16S rRNA gene sequences in Crystal Geyser (with less than four mismatches; HUB1206 5'-GCCCTAGACATTCGGACC-3'). The probe was 5' and 3' labeled with Cy3, while the already established probe for Altiarchaeota [23] was dual-labeled with the fluorescence-dye Atto488 (biomers.net, Ulm, Germany).

The FISH protocol was carried out as performed earlier for Altiarchaeota [23] using 0.005% SDS (w/v) and 15% deionized formamide (v/v) [24] and a probe concentration of 1 pmol/µL). Cells were counter-stained with 5 µL DAPI staining solution (DAPI solution: 50 mM EDTA pH 8.0, 0.6M Na-acetate pH 4,7, 20 ng/mL DAPI solution; 1:15 diluted in washing buffer) for 4 min at RT. The samples were examined using a Zeiss microscope (Carl Zeiss, Jena, Germany) with appropriate filter sets for Cy3, DAPI and Atto488 and a 100x Plan Apochromat objective.

The negative control for the Ca. *H. crystalense* probe was performed on biofilm samples collected from the Islinger Mühlbach, where Altiarchaeota show an extremely high abundance (~90% of the community) and of which a detailed metagenome exists [4]. The conditions for FISH were identical as described above. The probe showed no hybridization signal with Altiarchaeota or any other organisms (other Archaea or Bacteria) in the ecosystem (*Fig. 1-VI*) displaying the high specificity of the probe (as determined *in silico*) and no cross-hybridizations with Altiarchaeota or other Bacteria in the sample.

2. Supplementary Tables

Table S1 | Gene products of Ca. *A. hamiconexum* CG that could produce substrates for the metabolism of Ca. *H. chrystalense* as displayed in main *Fig. 2*. Enzymes in grey have been re-annotated manually (see Supplementary Methods and Table S3).

No. in Fig. 2	Label	Gene	Gene product	Product potentially used by Huberiarchaeum
1	ALTICG_v1_1430002	pdxT	pyridoxal 5'-phosphate synthase	PLP
1	ALTICG_v1_11110003	pdxT	pyridoxal 5'-phosphate synthase (fragment)	
1	ALTICG_v1_450003	pdxS	pyridoxal 5'-phosphate synthase	
1	ALTICG_v1_15950001	pdxS	pyridoxal 5'-phosphate synthase (modular protein)	
2	ALTICG_v1_120002	ribB	3,4-dihydroxy-2-butanone 4-phosphate synthase	FAD
3	ALTICG_v1_2080006		6,7-dimethyl-8-ribityllumazine synthase (modular protein)	
4	ALTICG_v1_220004	ribC	riboflavin synthase	
4	ALTICG_v1_15930002	ribC	riboflavin synthase (fragment)	
5	ALTICG_v1_10003		putative CTP-dependent riboflavin kinase	
6	ALTICG_v1_800016	ribL	FAD synthase	
7	ALTICG_v1_14400005		putative 5-amino-6-(5-phosphoribosylamino)uracil reductase	
8	ALTICG_v1_8770004		Diaminohydroxyphosphoribosylaminopyrimidine reductase	
9	ALTICG_v1_14400005		2,5-diamino-6-ribosylamino-4(3H)-pyrimidinone 5'-phosphate reductase	
10	ALTICG_v1_780003	nadX	putative aspartate dehydrogenase	NAD(P)$^+$
11	ALTICG_v1_1640001	nadA	quinolinate synthase A	
12	ALTICG_v1_2270011	nadC	putative nicotinate-nucleotide pyrophosphorylase [carboxylating]	
13	ALTICG_v1_1540004		nicotinamide nucleotide adenylyltransferase	
14	ALTICG_v1_990003	nadE	NH_3-dependent NAD$^+$ synthetase	
15	ALTICG_v1_7580003	nadK	NAD$^+$ kinase	
16	ALTICG_v1_16620001		Nicotinate-nucleotide-dimethylbenzimidazole phosphoribosyltransferase (fragment)	
17	ALTICG_v1_10940006		GTP cyclohydrolase MptA	methylene-THF
18	ALTICG_v1_17060006		putative alkaline phosphatase	
19	ALTICG_v1_1450017	trxB	Thioredoxin reductase	
19	ALTICG_v1_18720001		Thioredoxin reductase (fragment)	methylene-THF
20	ALTICG_v1_15630006	mptE	6-hydroxymethyl-7,8-dihydropterin pyrophosphokinase	
21	ALTICG_v1_9730008		Dihydropteroate synthase	
22	ALTICG_v1_14240002		putative dihydrofolate synthase/tetrahydrofolate synthase	
23	ALTICG_v1_2070006		GTP cyclohydrolase I FolE2	
24	ALTICG_v1_15240002		putative anthranilate/para-aminobenzoate synthase component I	
25	ALTICG_v1_12630003		putative aminodeoxychorismate lyase	
26	ALTICG_v1_11410004		putative folylpolyglutamate synthase	
27	ALTICG_v1_2120011	glyA	serine hydroxymethyltransferase	
28	ALTICG_v1_11270005		putative bifunctional NADP-dependent methylenetetrahydromethanopterin dehydrogenase /methylenetetrahydrofolate dehydrogenase	
28	ALTICG_v1_1440001		Methylenetetrahydrofolate dehydrogenase	
29	ALTICG_v1_1800003	folD	bifunctional methylenetetrahydrofolate dehydrogenase/methenyltetrahydrofolate cyclohydrolase	
29	ALTICG_v1_11270006		putative methenyltetrahydromethanopterin cyclohydrolase	
29	ALTICG_v1_11270006		methenyltetrahydromethanopterin cyclohydrolase (fragment)	
30	ALTICG_v1_350005	purU	Formyltetrahydrofolate deformylase	
31	ALTICG_v1_14850007	metF	methylenetetrahydrofolate reductase	
32	ALTICG_v1_12010007		Putative tungsten-containing formylmethanofuran dehydrogenase subunit A	

32	ALTICG_v1_14350006		putative molybdenum-containing formylmethanofuran dehydrogenase 1 subunit C	
32	ALTICG_v1_390006	fwdB	tungsten-containing formylmethanofuran dehydrogenase 2 subunit B	
32	ALTICG_v1_10970017		putative tungsten-containing formylmethanofuran dehydrogenase 2 subunit C	
32	ALTICG_v1_12750017		formylmethanofuran dehydrogenase subunit C	
32	ALTICG_v1_12010009		Putative tungsten-containing formylmethanofuran dehydrogenase subunit D	
33	ALTICG_v1_790002	ffsA	Formylmethanofuran-tetrahydromethanopterin formyltransferase	
34	ALTICG_v1_9060004		putative Adenylate cyclase	
35	ALTICG_v1_10330002		putative dihydromethanopterin reductase	
36	ALTICG_v1_17310002		putative acetyl-CoA synthetase	Acetyl-CoA for molecular building blocks
37	ALTICG_v1_17800001		putative CO dehydrogenase/acetyl-CoA synthase subunit alpha 1	
37	ALTICG_v1_19430001		putative CO dehydrogenase/acetyl-CoA synthase subunit alpha 2	
37	ALTICG_v1_11000009		CO dehydrogenase/acetyl-CoA synthase subunit beta 2	
37	ALTICG_v1_10980002		putative CO dehydrogenase/acetyl-CoA synthase subunit gamma	
37	ALTICG_v1_110003	cdhD	CO dehydrogenase/acetyl-CoA synthase subunit delta	
38	ALTICG_v1_16180001		formate dehydrogenase, nitrate-inducible, iron-sulfur subunit (fragment)	
38	ALTICG_v1_17400007		putative formate dehydrogenase subunit alpha	
38	ALTICG_v1_16180001		putative formate dehydrogenase subunit beta	
38	ALTICG_v1_1900004		formate dehydrogenase family accessory protein FdhD	
39	ALTICG_v1_12180007		gamma carbonic anhydrase family protein	
39	ALTICG_v1_12180007		carbonic anhydrase	
40	ALTICG_v1_12340001		putative lactate dehydrogenase	
41	ALTICG_v1_1540003	porA	pyruvate ferredoxin oxidoreductase subunit alpha/ pyruvate synthase subunit porA	
41	ALTICG_v1_14030010	porB	putative pyruvate ferredoxin oxidoreductase subunit beta/ pyruvate synthase subunit porB	
41	ALTICG_v1_14030010	porB	putative pyruvate ferredoxin oxidoreductase subunit beta/ pyruvate synthase subunit porB (fragment)	
41	ALTICG_v1_8190001	porC	pyruvate ferredoxin oxidoreductase subunit gamma/ pyruvate synthase subunit porC	
41	ALTICG_v1_11490003	porD	pyruvate ferredoxin oxidoreductase subunit delta/ pyruvate synthase subunit porD	
42	ALTICG_v1_570001	ppsA	phosphoenolpyruvate synthase	DHAP G1P
43	ALTICG_v1_2330001	eno	enolase	
44	ALTICG_v1_2270003	apgM	2,3-bisphosphoglycerate-independent phosphoglycerate mutase 1	
44	ALTICG_v1_10720019		2,3-bisphosphoglycerate-independent phosphoglycerate mutase 1 (fragment)	
44	ALTICG_v1_2490001		phosphoglycerate mutase	
45	ALTICG_v1_5680001	pgk	phosphoglycerate kinase	
45	ALTICG_v1_1630005		Phosphoglycerate kinase (fragment)	
46	ALTICG_v1_50009	gap	glycerinaldehyde-3-phosphate dehydrogenase	
47	ALTICG_v1_450012	tpiA	triosephosphate isomerase	
48	ALTICG_v1_2870001	fbp	bifunctional fructose-1,6-bisphosphate aldolase/phosphatase	G1P
48	ALTICG_v1_920002		Fructose-1,6-bisphosphate aldolase/phosphatase (fragment)	
49	ALTICG_v1_10090002	pfkB	putative 6-phosphofructokinase	
50	ALTICG_v1_10510014		Putative glucose-6-phosphate isomerase	
51	ALTICG_v1_11770006		putative transketolase N-terminal section	
51	ALTICG_v1_6930013		putative transketolase C-terminal section	
52	ALTICG_v1_1160006	tal	putative transaldolase	
53	ALTICG_v1_1180001	rpiA	Ribose-5-phosphate-Isomerase A	
54	ALTICG_v1_1910021	rpe	Ribulose-phosphate 3-epimerase	
55	ALTICG_v1_11640005		Ribose-phosphate pyrophosphokinase	GMP AMP
56	ALTICG_v1_1570023	purF	Amidophosphoribosyltransferase	
57	ALTICG_v1_70016	purD	phosphoribosylamine-glycine ligase	
58	ALTICG_v1_780009		Phosphoribosylglycinamide formyltransferase	
59	ALTICG_v1_300002	purL	phosphoribosylformylglycinamidine synthase subunit purL	

59	ALTICG_v1_ 2610002		phosphoribosylformylglycinamidine synthase subunit purL (fragment)	
59	ALTICG_v1_780016	purQ	phosphoribosylformylglycinamidine synthase subunit purQ	
59	ALTICG_v1_18190001		phosphoribosylformylglycinamidine synthase subunit purQ (fragment)	
60	ALTICG_v1_190011	purM	phosphoribosylformylglycinamidine cyclo-ligase	
61	ALTICG_v1_1870002		putative phosphoribosylaminoimidazole carboxylase	
62	ALTICG_v1_780017	purC	phosphoribosylaminoimidazole-succinocarboxamide synthase	
63	ALTICG_v1_10780018	purB	Adenylosuccinate lyase	
64	ALTICG_v1_11200001	purH	Phosphoribosylaminoimidazolecarboxamide formyltransferase/ IMP cyclohydrolase	
65	ALTICG_v1_10580005		putative IMP dehydrogenase	
66	ALTICG_v1_10250001	guaAB	GMP synthase [glutamine-hydrolyzing] subunit B	
67	ALTICG_v1_11170008	purA	Adenylosuccinate synthetase	
68	ALTICG_v1_10860008	adkA	Adenylate kinase	UTP/dUTP ATP/dATP GTP/dGTP dCTP
69	ALTICG_v1_1460001	ndk	nucleoside diphosphate kinase	
70	ALTICG_v1_17110001		putative ribonucleoside triphosphate reductase	
70	ALTICG_v1_2190001		Anaerobic ribonucleoside-triphosphate reductase activating protein	
71	ALTICG_v1_800002	carB	carbamoyl-phosphate synthase large chain, C-terminal section	UMP
71	ALTICG_v1_1570010	carB	carbamoyl-phosphate synthase large chain, N-terminal section	
71	ALTICG_v1_141001	carA	carbamoyl-phosphate synthase small chain	
72	ALTICG_v1_2430007	pyrB	aspartate carbamoyltransferase	
72	ALTICG_v1_2240010	pyrI	Aspartate carbamoyltransferase regulatory chain	
73	ALTICG_v1_3840006	pyrC	dihydroorotase	
75	ALTICG_v1_1680004	pyrD	dihydroorotate dehydrogenase B (NAD(+)), catalytic subunit	
75	ALTICG_v1_120009		dihydroorotate dehydrogenase electron transfer subunit	
75	ALTICG_v1_910004	pyrE	orotate phosphoribosyltransferase	
76	ALTICG_v1_10510002	pyrF	orotidine-5'-phosphate decarboxylase	
77	ALTICG_v1_150001	pyrH	uridylate kinase	dUMP/UTP
78	ALTICG_v1_990013	tmk	putative thymidylate kinase	dTTP
78	ALTICG_v1_1100004	tmk	dTMP kinase	
79	ALTICG_v1_860003	thyX	Flavin-dependent thymidylate synthase	dTMP
80	ALTICG_v1_16450006	pyrG	CTP synthase	CTP
80	ALTICG_v1_16000003	pyrG	CTP synthase (fragment)	
81	ALTICG_v1_620001	dcd	putative dCTP deaminase	dUTP
82	ALTICG_v1_1620001	cmk	cytidylate kinase	CTP/dCTP
83	ALTICG_v1_13890009	nuoI	NADH-quinone oxidoreductase subunit I	ATP
83	ALTICG_v1_1040002	nuoB	NADH-quinone oxidoreductase subunit B	
83	ALTICG_v1_1040003	nuoCD	NADH-quinone oxidoreductase subunit C/D	
83	ALTICG_v1_13890007		NADH-quinone oxidoreductase subunit D (modular protein)	
83	ALTICG_v1_1040004	nuoH	NADH-quinone oxidoreductase subunit H	
83	ALTICG_v1_2180014	nuoK	NADH-quinone oxidoreductase subunit K	
85	ALTICG_v1_16970009		ADP-ribose pyrophosphatase (fragment)	
86	ALTICG_v1_15230005		putative adenosine specific kinase	
87	ALTICG_v1_1760006		putative 3-hydroxy-3-methylglutaryl-coenzyme A synthase	IPP
88	ALTICG_v1_11110019		Acetyl-CoA acetyltransferase	
89	ALTICG_v1_15560016	hmgA	hydroxymethylglutaryl-CoA reductase	
90	ALTICG_v1_1070001	mvk	mevalonate kinase	
91	ALTICG_v1_1560003	mvaD	diphosphomevalonate decarboxylase	
92	ALTICG_v1_14030006		ferredoxin	ferredoxin
93	ALTICG_v1_1740003	fni	isopentenyl-diphosphate Delta-isomerase	
94	ALTICG_v1_3480004		prenyltransferase	
94	ALTICG_v1_6550010		prenyltransferase (fragment)	
95	ALTICG_v1_10370011		putative short chain isoprenyl diphosphate synthase	
96	ALTICG_v1_10240007		putative 2-ketoisovalerate ferredoxin oxidoreductase	
97	ALTICG_v1_15060007		Acylneuraminate cytidylyltransferase (fragment)	Activated sugars
98	ALTICG_v1_5710001	egsA	NAD(P)-dependent glycerol-1-phosphate dehydrogenase	

99	ALTICG_v1_12830001		Digeranylgeranylglyceryl phosphate synthase	
100	ALTICG_v1_2830001		putative digeranylgeranylglycerophospholipid reductase	
101	ALTICG_v1_1720015	uppS	Tritrans,polycis-undecaprenyl-diphosphate synthase (geranylgeranyl-diphosphate specific)	
103	ALTICG_v1_180001		malate dehydrogenase	
104	ALTICG_v1_2200004	pckG	phosphoenolpyruvate carboxykinase [GTP]	
105	ALTICG_v1_14450004		putative fumarate hydratase class II	
105	ALTICG_v1_16010001		fumarate hydratase class II (fragment)	
106	ALTICG_v1_400003		Aconitate hydratase	
107	ALTICG_v1_1010024	icd	Isocitrate dehydrogenase [NADP+]	
108	ALTICG_v1_1930005		Succinyl-CoA synthetase subunit alpha	
109	ALTICG_v1_17410006		Putative CoB-CoM heterodisulfide reductase subunit B	
109	ALTICG_v1_13530010		Heterodisulfide reductase subunit B (fragment)	
109	ALTICG_v1_13530007		putative CoB-CoM heterodisulfide,ferredoxin reductase subunit A	
110	ALTICG_v1_4310002		putative bifunctional amino acid acetyltransferase/glutamate N-acetyltransferase	Arg
111	ALTICG_v1_11220008	argB	acetylglutamate kinase	
112	ALTICG_v1_2420003	argC	N-acetyl-gamma-glutamyl-phosphate reductase	
112	ALTICG_v1_17780013		N-acetyl-gamma-glutamyl-phosphate reductase (fragment)	
113	ALTICG_v1_2010003	argD	acetylornithine aminotransferase	
114	ALTICG_v1_14340003	argJ	glutamate N-acetyltransferase	
115	ALTICG_v1_1470017	argF	ornithine carbamoyltransferase	
116	ALTICG_v1_2490003	argG	argininosuccinate synthase	
116	ALTICG_v1_15110003		argininosuccinate synthase (fragment)	
117	ALTICG_v1_990011	argH	argininosuccinate lyase	
117	ALTICG_v1_14200008		argininosuccinate lyase (fragment)	
118	ALTICG_v1_10970009		Arginase	
119	ALTICG_v1_3900006	glnA	glutamine synthetase	
119	ALTICG_v1_15030004		glutamine synthetase (fragment)	
120	ALTICG_v1_15790002	phzB	Glutamine amidotransferase	Gln Glu Asp Asn
121	ALTICG_v1_2720003	gdhA	glutamate dehydrogenase, NADP-specific	
121	ALTICG_v1_16090004		glutamate dehydrogenase, NADP-specific (fragment)	
122	ALTICG_v1_310003	aspC	aspartate aminotransferase	
123	ALTICG_v1_2560007	ansB	asparagine synthase (Glutamine-hydrolyzing)	
123	ALTICG_v1_14390004		asparagine synthase (fragment)	
124	ALTICG_v1_990007	ansB	Aspartate ammonia-lyase	Asp homoserine Thr
124	ALTICG_v1_14450004		Aspartate ammonia-lyase (fragment)	
125	ALTICG_v1_10220001		Aspartate kinase (fragment)	
126	ALTICG_v1_220003	asd	aspartate-semialdehyde dehydrogenase	
127	ALTICG_v1_1950007	hom	Homoserine dehydrogenase	
128	ALTICG_v1_350002	thrC	threonine synthase	
129	ALTICG_v1_11920007	cimA	(R)-citramalate synthase	Val Leu Ile
130	ALTICG_v1_1880008	leuC	3-isopropylmalate dehydratase large subunit	
130	ALTICG_v1_13380003	leuD	3-isopropylmalate dehydratase small subunit 2	
130	ALTICG_v1_4780014	leuD	Isopropylmalate/citramalate isomerase small subunit	
131	ALTICG_v1_7880008	leuB	3-isopropylmalate dehydrogenase	
132	ALTICG_v1_15550018	ilvB	putative acetolactate synthase large subunit	
132	ALTICG_v1_1010008	ilvH	putative acetolactate synthase small subunit	
133	ALTICG_v1_1910009	ilvC	Ketol-acid reductoisomerase (NADP(+))	
133	ALTICG_v1_15580001		Ketol-acid reductoisomerase (NADP(+)) (fragment)	
134	ALTICG_v1_1450020	ilvD	Dihydroxy-acid dehydratase	
135	ALTICG_v1_1720003	ilvE	putative branched-chain-amino-acid aminotransferase	
136	ALTICG_v1_2050003	leuA	putative 2-isopropylmalate synthase	
136	ALTICG_v1_8980008		2-isopropylmalate synthase (fragment)	
137	ALTICG_v1_800012	dapA	4-hydroxy-tetrahydrodipicolinate synthase	Lys

138	ALTICG_v1_2490005	dapB	4-hydroxy-tetrahydrodipicolinate reductase	
139	ALTICG_v1_760001	dapL	LL-diaminopimelate aminotransferase	
140	ALTICG_v1_10940005	dapF	Diaminopimelate epimerase	
141	ALTICG_v1_10050010	lysA	Diaminopimelate decarboxylase	
142	ALTICG_v1_1080003	pdaD	putative pyruvoyl-dependent arginine decarboxylase	
143	ALTICG_v1_10970009	speB	agmatinase	
143	ALTICG_v1_17630001		Agmatinase (fragment)	
144	ALTICG_v1_120010	hisG	ATP phosphoribosyltransferase	His
145	ALTICG_v1_11110023		Putative phosphoribosyl-ATP pyrophosphohydrolase/ phosphoribosyl-AMP cyclohydrolase	
146	ALTICG_v1_1900017		Phosphoribosyl-AMP cyclohydrolase	
147	ALTICG_v1_13830005	hisA	1-(5-phosphoribosyl)-5-[(5-phosphoribosylamino) methylideneamino] imidazole-4-carboxamide isomerase	
148	ALTICG_v1_10220016		putative imidazoleglycerol-phosphate synthase cyclase subunit	
148	ALTICG_v1_18360002		putative imidazoleglycerol-phosphate synthase	
149	ALTICG_v1_10220014		Imidazoleglycerol-phosphate dehydratase	
150	ALTICG_v1_10460002	hisC	Histidinol-phosphate aminotransferase	
151	ALTICG_v1_1630001	hisD	histidinol dehydrogenase	
152	ALTICG_v1_15820005	aroB	3-dehydroquinate synthase	Trp Phe Tyr
153	ALTICG_v1_10720016		putative 3-dehydroquinate dehydratase	
154	ALTICG_v1_1610003	aroE	Shikimate dehydrogenase (NADP(+))	
155	ALTICG_v1_14980003	aroK	Shikimate kinase	
156	ALTICG_v1_12030009	aroA	3-phosphoshikimate 1-carboxyvinyltransferase	
157	ALTICG_v1_390001	aroC	chorismate synthase	
158	ALTICG_v1_17100001		chorismate mutase (fragment)	
159	ALTICG_v1_800018	pheA	Prephenate dehydratase	
160	ALTICG_v1_2500003		Prephenate dehydrogenase	
160	ALTICG_v1_12940002		putative arogenate/prephenate dehydrogenase (fragment)	
161	ALTICG_v1_14840010		aromatic amino acid aminotransferase	
162	ALTICG_v1_15810007	mfnA	L-tyrosine/L-aspartate decarboxylase	
162	ALTICG_v1_15270005		L-aspartate decarboxylase (fragment)	
163	ALTICG_v1_11290002		Phenazine-specific anthranilate synthase component I	
164	ALTICG_v1_720002	trpD	Anthranilate phosphoribosyltransferase	
165	ALTICG_v1_13630003	trpC	Indole-3-glycerol phosphate synthase	
166	ALTICG_v1_2400007	trpA	tryptophan synthase alpha chain	
166	ALTICG_v1_2260002	trpB	tryptophan synthase beta subunit	
167	ALTICG_v1_14850006	metE	5-methyltetrahydropteroyltriglutamate-homocysteine methyltransferase	SAM
168	ALTICG_v1_1740011	mat	S-adenosylmethionine synthase	
168	ALTICG_v1_17700001		putative Methionine adenosyltransferase	
170	ALTICG_v1_380003	ahcY	adenosylhomocysteinase	
171	ALTICG_v1_9220013	mqnC	Cyclic dehypoxanthine futalosine synthase	SAM
172	ALTICG_v1_2920007	pcm	Protein-L-isoaspartate O-methyltransferase	
173	ALTICG_v1_14410003	dphB	Diphthine synthase	
174	ALTICG_v1_16240001		Phosphomethylpyrimidine synthase (fragment)	SAM
175	ALTICG_v1_13910009		putative homoserine O-acetyltransferase	Ser Ala Cys
176	ALTICG_v1_2350004	serB	Phosphoserine phosphatase	
177	ALTICG_v1_2470003	iscS	Cysteine desulfurase	
178	ALTICG_v1_19270004		putative serine acetyltransferase	
179	ALTICG_v1_550003	cobT	Nicotinate-nucleotide-dimethylbenzimidazole phosphoribosyltransferase	AdoCbl
180	ALTICG_v1_11320004		cobalt chelatase	
181	ALTICG_v1_140011	cobD	Cobalamin biosynthesis protein CobD	
182	ALTICG_v1_140005		Cob(I)yrinic acid a,c-diamide adenosyltransferase	
183	ALTICG_v1_2500001		Bifunctional adenosylcobinamide kinase/adenosylcobinamide-phosphate guanylyltransferase	
184	ALTICG_v1_1810001	cobS	Adenosylcobinamide-GDP ribazoletransferase	

185	ALTICG_v1_2780010		putative UTP-glucose-1-phosphate uridylyltransferase	Activated sugars G1P
185	ALTICG_v1_1610011		UTP-glucose-1-phosphate uridylyltransferase (fragment)	
186	ALTICG_v1_890014		putative UDP-glucose 4-epimerase	
187	ALTICG_v1_40007	tuaD	UDP-glucose-6-dehydrogenase	
188	ALTICG_v1_40008		putative UDP-D-glucuronate decarboxylase	
189	ALTICG_v1_14630003		putative UDP-4-amino-4-deoxy-L-arabinose-oxoglutarate aminotransferase	
190	ALTICG_v1_800023		bifunctional phosphoglucomutase/phosphomannomutase	
191	ALTICG_v1_18750004	xanB	mannose-6-phosphate isomerase/mannose-1-phosphate guanylyltransferase	
192	ALTICG_v1_1610007	strD	glucose-1-phosphate thymidylyltransferase	
192	ALTICG_v1_7310001		glucose-1-phosphate thymidylyltransferase (fragment)	
193	ALTICG_v1_10970018		putative glucose-1-phosphate adenylyltransferase	
194	ALTICG_v1_1600004	rfbF	glucose-1-phosphate cytidylyltransferase	
195	ALTICG_v1_1360008	tpsp	Alpha,alpha-trehalose-phosphate synthase [UDP-forming] / trehalose-6-phosphate phosphatase	
196	ALTICG_v1_6330013	gmd	GDP-D-mannose 4,6-dehydratase, NAD(P)-binding	
197	ALTICG_v1_8660002		GDP-L-fucose synthase (fragment)	
198	ALTICG_v1_2740002	rmlC	dTDP-4-dehydrorhamnose 3,5-epimerase	
199	ALTICG_v1_17460001		glucosamine-fructose-6-phosphate aminotransferase (fragment)	
200	ALTICG_v1_12370014	glmM	phosphoglucosamine mutase	
201	ALTICG_v1_2100006	glmU	UDP-N-acetylglucosamine pyrophosphorylase / Glucosamine-1-phosphate N-acetyltransferase	
202	ALTICG_v1_13920009		UDP-N-acetylglucosamine pyrophosphorylase / Glucosamine-1-phosphate N-acetyltransferase (fragment)	
203	ALTICG_v1_510005	wecB	UDP-N-acetylglucosamine 2-epimerase	
203	ALTICG_v1_15990003		UDP-N-acetylglucosamine 2-epimerase (fragment)	
204	ALTICG_v1_14630006		UDP-N-acetylglucosamine 3-dehydrogenase (fragment)	
205	ALTICG_v1_18870008		dTDP-glucose 4,6-dehydratase (fragment)	
205	ALTICG_v1_1610005	rmlB	dTDP-glucose 4,6 dehydratase, NAD(P)-binding	
206	ALTICG_v1_510003	wecC	UDP-N-acetyl-D-mannosamine dehydrogenase	
206	ALTICG_v1_16820004		UDP-N-acetyl-D-glucosamine 6-dehydrogenase (fragment)	
207	ALTICG_v1_10760013		putative dTDP-4-dehydrorhamnose reductase	
208	ALTICG_v1_11690017	pseH	UDP-4-amino-4, 6-dideoxy-N-acetyl-beta-L-altrosamine N-acetyltransferase	
209	ALTICG_v1_19330001	amC	Undecaprenyl-phosphate 4-deoxy-4-formamido-L-arabinose transferase	
210	ALTICG_v1_1790001		putative endoglucanase/ cellulase/ putative peptidase M42	
211	ALTICG_v1_60004		putative alpha-amylase	
212	ALTICG_v1_3110006		alpha-1,4 glucan phosphorylase	
213	ALTICG_v1_11570001		Glycogen debranching protein	
214	ALTICG_v1_11290001		putative glycogen [starch] synthase	glycogen
215	ALTICG_v1_3550008		putative CDP-4-dehydro-6-deoxy-D-gulose 4-reductase	Activated sugars
216	ALTICG_v1_10210015		putative Ferredoxin-NADP reductase	red. ferredoxin
217	ALTICG_v1_13890016	arsC	Arsenate reductase	
218	ALTICG_v1_13890012	arsM	Arsenite methyltransferase	
219	ALTICG_v1_13890017	arsB	Arsenite resistance protein ArsB	
220	ALTICG_v1_11110015		putative archaeal A1AO-type ATP synthase, subunit K	ATP
220	ALTICG_v1_14070002		putative archaeal A1AO-type ATP synthase, subunit B	
220	ALTICG_v1_15150001		putative archaeal A1AO-type ATP synthase, subunit A	
220	ALTICG_v1_10430022		putative archaeal A1AO-type ATP synthase, subunit D	
220	ALTICG_v1_12040009		putative archaeal A1AO-type ATP synthase, subunit C	
220	ALTICG_v1_16550006		putative archaeal A1AO-type ATP synthase, subunit I	

Table S2 | Gene products of Ca. *H. chrystalense* that could potentially use substrates provided by Ca. *A. hamiconexum* as displayed in Figure 2. Enzymes in grey have been re-annotated manually (see Supplementary Methods and Table S3).

No. In Fig. 2	Label	Gene	Gene product	Component potentially derived from Altiarchaeum
19	HUBERARCH_v1_220006	trxB	Thioredoxin reductase	NAD(P)H
19	HUBERARCH_v1_4870001		Thioredoxin reductase (fragment)	NAD(P)H
69	HUBERARCH_v1_4750008	ndk	Nucleoside diphosphate kinase	ATP/GTP
70	HUBERARCH_v1_100006	nrdD	anaerobic ribonucleoside triphosphate reductase	AdoCbl
78	HUBERARCH_v1_230004	tmk	putative thymidylate kinase	ATP/GTP
79	HUBERARCH_v1_1440004		Putative thymidylate synthase	methylene-THF
80	HUBERARCH_v1_260014	pyrG	CTP synthase	ATP/GTP
84	HUBERARCH_v1_110006		putative CMP/dCMP deaminase zinc-binding protein, dCMP deaminase	Zn^{2+}
93	HUBERARCH_v1_370010	idi	Isopentenyl-diphosphate delta-isomerase 2	
94	HUBERARCH_v1_80001		Geranylgeranyl diphosphate synthase	
98	HUBERARCH_v1_3540004	egsA	NAD(P)-dependent glycerol-1-phosphate dehydrogenase	NAD(P)H
98	HUBERARCH_v1_1470004		NAD(P)-dependent glycerol-1-phosphate dehydrogenase (fragment)	NAD(P)H
100	HUBERARCH_v1_1430005		putative digeranylgeranylglycerophospholipid reductase	reduced ferredoxin
102	HUBERARCH_v1_800015	ytsJ	putative NAD-dependent malic enzyme 4	NAD(P)H
103	HUBERARCH_v1_10014		putative malic protein NAD-binding protein, malate dehydrogenase (Oxaloacetate-decarboxylating)	NAD(P)H
103	HUBERARCH_v1_10014	ytsJ	putative malate dehydrogenase	NAD(P)H
118	HUBERARCH_v1_2100015		arginase	
122	HUBERARCH_v1_100004		putative aspartate aminotransferase	PLP
123	HUBERARCH_v1_110022		putative asparagine synthase	
143	HUBERARCH_v1_3660016		putative agmatinase	
159	HUBERARCH_v1_100003		Prephenate dehydratase	
166	HUBERARCH_v1_1170012		putative tryptophan synthase alpha chain	PLP
169	HUBERARCH_v1_4370002		DNA (Cytosine-5-)-methyltransferase	SAM
172	HUBERARCH_v1_950023		Protein-L-isoaspartate O-methyltransferase	SAM
173	HUBERARCH_v1_220013	dph	Diphthine synthase	SAM
177	HUBERARCH_v1_630002	iscS	cysteine desulfurylase	PLP
186	HUBERARCH_v1_860003		putative UDP-glucose 4-epimerase	
192	HUBERARCH_v1_2660001	strD	glucose-1-phosphate thymidylyltransferase	dTTP
193	HUBERARCH_v1_3470001		putative glucose-1-phosphate adenylyltransferase	ATP
194	HUBERARCH_v1_520002	rfbF	Glucose-1-phosphate cytidylyltransferase	CTP
196	HUBERARCH_v1_520006		GDP-mannose 4,6-dehydratase	
198	HUBERARCH_v1_520004	rfbC	dTDP-4-dehydrorhamnose 3,5-epimerase	
198	HUBERARCH_v1_860002	rmlC	dTDP-4-dehydrorhamnose 3,5-epimerase	
203	HUBERARCH_v1_360004		UDP-N-acetylglucosamine 2-epimerase (Non-hydrolyzing)	
203	HUBERARCH_v1_2160021		UDP-N-acetylglucosamine 2-epimerase (fragment)	
205	HUBERARCH_v1_960005	rmlB	dTDP-glucose 4,6-dehydratase, NAD(P)-binding	
207	HUBERARCH_v1_2660002		putative dTDP-4-dehydrorhamnose reductase	
210	HUBERARCH_v1_1780008		putative endoglucanase/ cellulose/ putative peptidase M42	
215	HUBERARCH_v1_2860003		CDP-4-dehydro-6-deoxy-D-gulose 4-reductase	
221	HUBERARCH_v1_4290002		DNA alkylation repair protein	
	HUBERARCH_v1_4600012		DNA helicase UvrD	
	HUBERARCH_v1_4520009	radA	DNA repair and recombination protein RadA	
	HUBERARCH_v1_4470025	radB	DNA repair and recombination protein RadB	
	HUBERARCH_v1_4350016	lig	DNA ligase	

222	HUBERARCH_v1_4570037	lon	Archaeal Lon protease	
	HUBERARCH_v1_2850003	htpX	Protease HtpX homolog	
	HUBERARCH_v1_3710005		Proteasome endopeptidase complex	
	HUBERARCH_v1_4860003	pan	Proteasome-activating nucleotidase	
	HUBERARCH_v1_4470021	rrp	Exosome complex component Rrp41	
	HUBERARCH_v1_4350010		Metallopeptidase	
223	HUBERARCH_v1_4280019	cdc6	ORC1-type DNA replication protein 1	
	HUBERARCH_v1_4360019		Replication factor C large subunit (fragment)	
	HUBERARCH_v1_4610004	rfcS	Replication factor C small subunit	
	HUBERARCH_v1_240025	polC	DNA polymerase II large subunit	
	HUBERARCH_v1_1400015	polB	putative DNA polymerase II small subunit	
224	HUBERARCH_v1_4780003	rpoE	DNA-directed RNA polymerase subunit E'	
	HUBERARCH_v1_150003	rpoH	DNA-directed RNA polymerase subunit H	
	HUBERARCH_v1_4640001		DNA-directed RNA polymerase subunit N	
	HUBERARCH_v1_4320008		DNA-directed RNA polymerase subunit P (fragment)	
	HUBERARCH_v1_4380029	spt	Transcription elongation factor Spt4	
	HUBERARCH_v1_4470024		Transcription elongation factor Spt5	
	HUBERARCH_v1_520007		NarL family transcriptional regulator	
	HUBERARCH_v1_4280033	tfs	Transcription factor S	
	HUBERARCH_v1_850001		Transcriptional regulator	
225	HUBERARCH_v1_4420009		Protein translation factor SUI1 homolog	
	HUBERARCH_v1_4710005		Ribosome assembly factor SBDS	
	HUBERARCH_v1_4820004		Translation initiation factor IF-1A	
	HUBERARCH_v1_1800003		Translation initiation factor IF-2 subunit beta	
	HUBERARCH_v1_1180003		putative translation initiation factor 2 subunit gamma	
	HUBERARCH_v1_4430014	eif5A	Translation initiation factor IF-5A	
	HUBERARCH_v1_4390027	prf	Peptide chain release factor 1	
	HUBERARCH_v1_4390022	tuf	Elongation factor 1-alpha	
	HUBERARCH_v1_4520006	fusA	Elongation factor 2	
	HUBERARCH_v1_4690004		Nascent polypeptide-associated complex protein	
	HUBERARCH_v1_3060007	iscU	scaffold protein	
	HUBERARCH_v1_4500005	alaS	Alanine--tRNA ligase	
	HUBERARCH_v1_3590030		Alanyl-tRNA editing protein AlaX	
	HUBERARCH_v1_3590030		Alanyl-tRNA editing protein AlaX-M (fragment)	
	HUBERARCH_v1_4420021	argS	Arginine--tRNA ligase	
	HUBERARCH_v1_70012	aspS	Aspartate--tRNA(Asp) ligase	
	HUBERARCH_v1_4640004	gltX	Glutamate--tRNA ligase	
	HUBERARCH_v1_4390026	glyQS	Glycine--tRNA ligase	
	HUBERARCH_v1_4720003	hisS	Histidine--tRNA ligase 1//Histidine--tRNA ligase	
	HUBERARCH_v1_4730001		Isoleucine--tRNA ligase	
	HUBERARCH_v1_4570039	leuS	Leucine--tRNA ligase	
	HUBERARCH_v1_3310003	lysS	Lysine--tRNA ligase	
	HUBERARCH_v1_4060001	metG	Methionine--tRNA ligase	
	HUBERARCH_v1_4550008		O-phospho-L-seryl-tRNA:Cys-tRNA synthase 1 (fragment)//O-phospho-L-seryl-tRNA:Cys-tRNA synthase	
	HUBERARCH_v1_4550005		O-phosphoserine--tRNA ligase	
	HUBERARCH_v1_4470010		Phenylalanine--tRNA ligase subunit beta	
	HUBERARCH_v1_4740002	proS	Proline--tRNA ligase	
	HUBERARCH_v1_4630008	serS	Serine--tRNA ligase	
	HUBERARCH_v1_4380006	thrS	Threonine--tRNA ligase	
	HUBERARCH_v1_4650006	trpS	Tryptophan--tRNA ligase	
	HUBERARCH_v1_4420012	tyrS	Tyrosine--tRNA ligase	
	HUBERARCH_v1_3850006	valS	Valine--tRNA ligase	
	HUBERARCH_v1_4470019	cca	CCA tRNA nucleotidyltransferase	

	HUBERARCH_v1_4670003	taw	S-adenosyl-L-methionine-dependent tRNA 4-demethylwyosine synthase//tRNA 4-demethylwyosine synthase (AdoMet-dependent)	
	HUBERARCH_v1_4390023	kae	tRNA N6-adenosine threonylcarbamoyltransferase//N(6)-L-threonylcarbamoyladenine synthase	
	HUBERARCH_v1_1990005	taw	tRNA(Phe) 7-((3-amino-3-carboxypropyl)-4-demethylwyosine(37)-N(4))-methyltransferase	
	HUBERARCH_v1_4390009		tRNA (cytidine(56)-2'-O)-methyltransferase	
	HUBERARCH_v1_4550008		O-phospho-L-seryl-tRNA:Cys-tRNA synthase 1 (fragment)//O-phospho-L-seryl-tRNA:Cys-tRNA synthase	
	HUBERARCH_v1_4280013	map	Methionine aminopeptidase	
226	HUBERARCH_v1_4360016		Cell division cycle protein 48 homolog AF_1297	
	HUBERARCH_v1_4400024		Cell division protein DedD	
	HUBERARCH_v1_4670006	ftsZ	Cell division protein FtsZ 1	
	HUBERARCH_v1_4390010	ftsZ	Cell division protein FtsZ 2	
	HUBERARCH_v1_4350004		Chromosomal protein MC1c	
	HUBERARCH_v1_4390019	topA	DNA topoisomerase 1	
	HUBERARCH_v1_1400025		Histone	
	HUBERARCH_v1_2580031		Histone (fragment)	
	HUBERARCH_v1_3900003		putative transposase	
227	HUBERARCH_v1_3390001		DNA adenine methylase	
	HUBERARCH_v1_4510001		Site-specific DNA-methyltransferase	
	HUBERARCH_v1_3390002		RNA methyltransferase	
228	HUBERARCH_v1_4310007		Beta-CASP ribonuclease aCPSF1	
	HUBERARCH_v1_1160001		Putative RNA-binding protein RbpB (fragment)	
	HUBERARCH_v1_4670005		putative snRNP Sm-like protein	
	HUBERARCH_v1_4510002		Restriction endonuclease subunit R	
	HUBERARCH_v1_3220009		Ribonuclease	
	HUBERARCH_v1_4380031	rnhB	Ribonuclease H	
	HUBERARCH_v1_3750016	rnp	Ribonuclease P protein component 2//Ribonuclease P	
	HUBERARCH_v1_4430009	rnz	Ribonuclease Z	
	HUBERARCH_v1_4660001		RNA 2',3'-cyclic phosphodiesterase	
	HUBERARCH_v1_4320005	flpA	Fibrillarin-like rRNA/tRNA 2'-O-methyltransferase	
	HUBERARCH_v1_1100002		Radical SAM protein	
	HUBERARCH_v1_3710008		Restriction endonuclease	
	HUBERARCH_v1_300001		Restriction endonuclease subunit M	
	HUBERARCH_v1_4470022		RNA-binding protein	
	HUBERARCH_v1_2860001		SAM-dependent methyltransferase	
	HUBERARCH_v1_3390007		Type I restriction endonuclease subunit M	
	HUBERARCH_v1_2730001		Type I restriction endonuclease subunit M	
	HUBERARCH_v1_4370001		Type II restriction endonuclease	
229	HUBERARCH_v1_3210001		Glycosyl transferase family	
	HUBERARCH_v1_4770003		Glycosyl transferase family 1	
	HUBERARCH_v1_3320001		Glycosyl transferase family 2	
	HUBERARCH_v1_4780002		Glycosyl transferase family 4	
	HUBERARCH_v1_3650003	agl	Low-salt glycan biosynthesis nucleotidyltransferase Agl11	

Table S3 | Cutoffs and taxonomy of the best hits of manually annotated enzymes (in grey in Table S1 and Table S2).

Number in Table S2	**% identity**	**taxonomy of the respective hit**
5	77.95	groundwater genome
7	47.70	Methanobacterium bryantii
18	82.23	HGW-Altiarchaeales-1
22	86.84	groundwater metagenome
24	40.46	Burkholderia lata (strain ATCC 17760 / DSM 23089 / LMG 22485 / NCIMB 9086 / R18194 / 383)
25	44.33	Bacillus subtilis (strain 168)
26	79.49	groundwater metagenome
28	39.66	Methylobacterium extorquens (strain ATCC 14718 / DSM 1338 / JCM 2805 / NCIMB 9133 / AM1)
29	90.57	groundwater metagenome
32	46.55-87.02	groundwater metagenome/ *Methanothermobacter wolfeii*
35	38.46	*Methanocaldococcus jannaschii* (strain ATCC 43067 / DSM 2661 / JAL-1 / JCM 10045 / NBRC 100440)
36	68.75	Candidatus Entotheonella factor
37	66.35-89.89	groundwater metagenome
38	90.00-91.08	groundwater metagenome
41	56.34	Methanococcus maripaludis X1
50	83.04	groundwater metagenome
61	91.89	groundwater metagenome
70	91.60	Candidatus Altiarchaeales archaeon A3
86	70.27	*Methanomassiliicoccales* archaeon PtaU1.Bin124
87	90.31	groundwater metagenome
95	86.24	groundwater metagenome
96	54.67	*Thermococcus guaymasensis*
100	80.08	groundwater metagenome
105	55.12	*Thermoflexus hugenholtzii* JAD2
109	43.93-87.5/	groundwater metagenome/ *Methanococcus maripaludis* (strain S2 / LL)
145	50.00	*Escherichia coli*
148	52.59-50.00	*Rhizobium etli/Thermoanaerobacter ethanolicus*
153	94.23	HGW-Altiarchaeales-2
175	45.69	*Methanococcoides burtonii* (strain DSM 6242 / NBRC 107633 / OCM 468 / ACE-M)
178	78.08	*Aciduliprofundum sp.* (strain MAR08-339)
188	49.64	*Nicotiana tabacum*
189	42.03	*Salmonella typhimurium* (strain LT2 / SGSC1412 / ATCC 700720)
193	84.44	groundwater metagenome
207	85.21	groundwater metagenome
210	47.48	Methanococcus maripaludis
214	85.95	groundwater metagenome
215	89.80	archaeon (Candidatus Huberarchaea) CG03_land_8_20_14_0_80_31_114
216	86.17	groundwater metagenome
220	80.68-93.84	groundwater genome
Number in Table S3	**% identity**	**taxonomy of the respective hit**
79	38.27	Parcubacteria group bacterium GW2011_GWF2_43_11
84	61.25	Berkelbacteria bacterium GW2011_GWE1_39_12
100	66.27	groundwater metagenome
103	55.36	Candidatus Peregrinibacteria bacterium GW2011_GWF2_43_17
143	53.70	*Methanobacterium* sp. PtaU1.Bin242
166	43.42	*Minicystis rosea*
186	45.71	*Arabidopsis thaliana*
193	90.12	groundwater metagenome

207	78.69	groundwater metagenome
210	48.99	*Methanobrevibacter olleyae*
225	53.33	Candidatus Pacearchaeota archaeon
226	73.10	Candidatus Methanoperedens nitroreducens

3. Supplementary Figures

Fig. S1 | **Maximum likelihood phylogenetic tree** inferred using IQTREE under the LG+C60+F+R model based on an alignment with 187 sequences and 4216 amino acid positions. Bootstrap support was inferred using a SH-like approximate likelihood ratio test and ultrafast bootstrap method and are reported at the respective branches. The first value refers to the results of the SH-like approximate likelihood ratio test and the second to the ultrafast bootstrap method. While the population genome of Ca. *Altiarchaeum hamiconexum* was not included in the phylogenetic analyses due to its high strain-level diversity, the Altiarchaeum sequence in bold face refers to a close relative of Ca. *Altiarchaeum hamiconexum*.

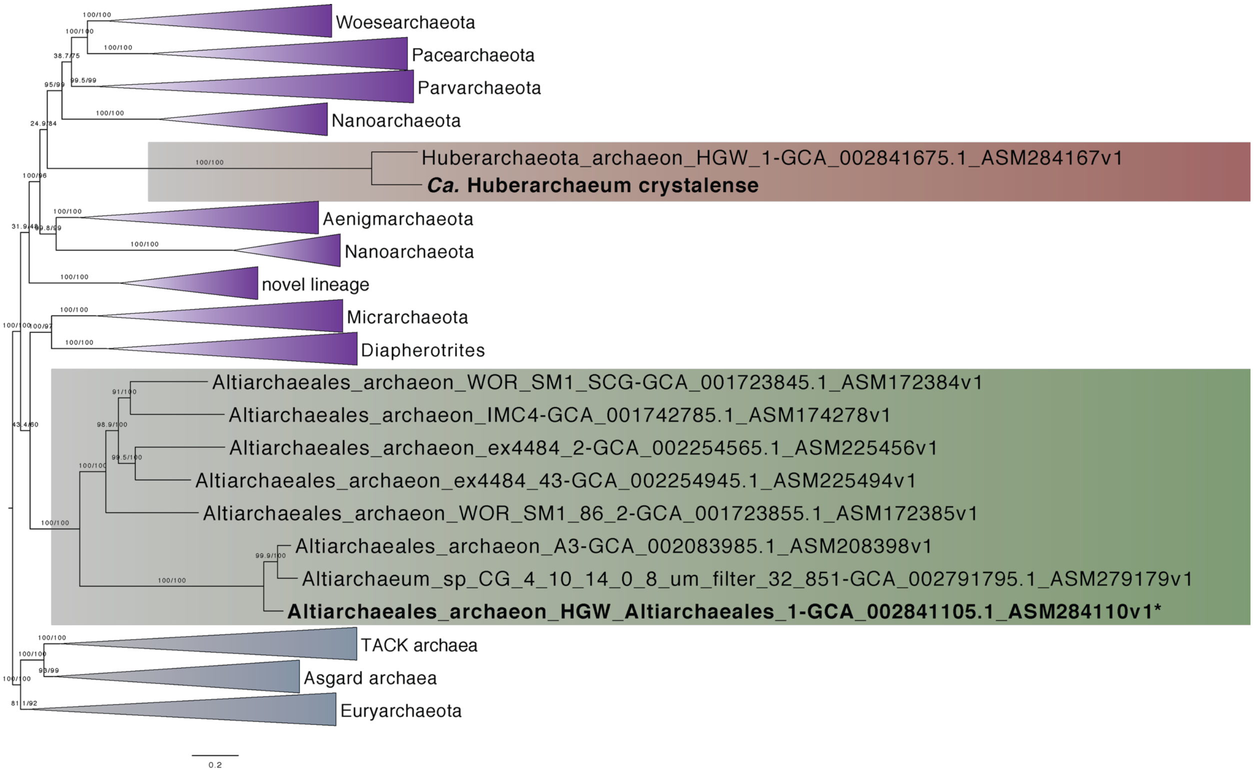

Fig. S2 | Proportionality analysis of 505 distinct genomes from Crystal Geyser. 10 of 504 organisms showed substantial ($\rho \geq 0.90$) proportional co-occurrence with Ca. Altiarchaeum CG, including Ca. Huberiarchaeum crystalense. **A**: Proportionality network of all proportional occurrences with $\rho \geq 0.90$. The edge lengths are arbitrary. Organism abundances co-occurring with those of Ca. Altiarchaeum CG are additionally highlighted. **B**: Read-normalized abundance of organisms with proportionality $\rho \geq 0.90$ compared to Ca. Altiarchaeum CG across 65 metagenomes. The color legend is shared across panels.

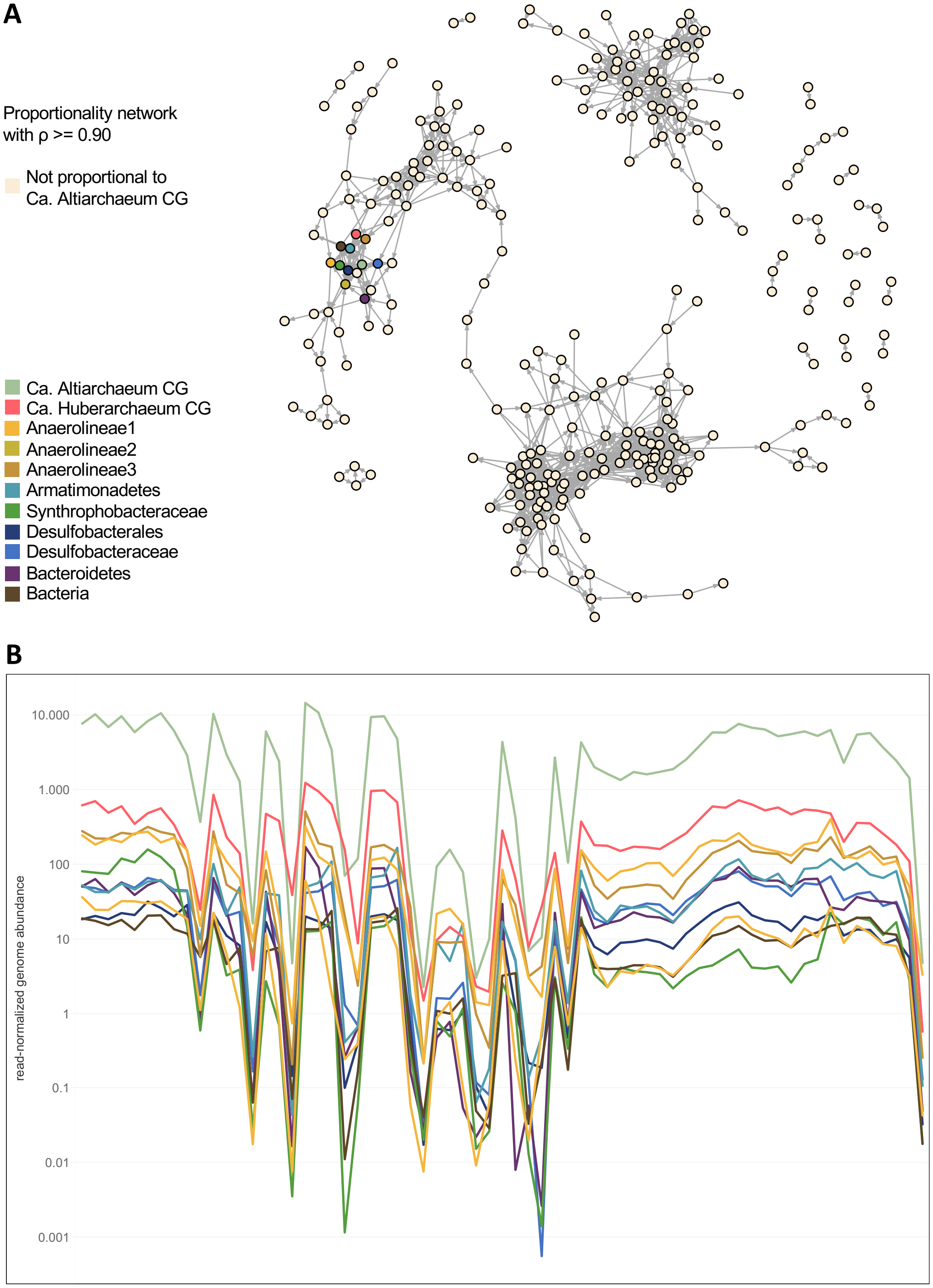

Fig. S3 | Ratios of relative abundances of Altiarchaeota and Huberarchaeota (based on stringent mapping of reads) across all samples. With the exception of a few smaller filters (0.1 µm and 0.2 µm), the ratio is about 11/1, i.e. eleven Ca. *Altiarchaeota* per one Ca. *Huberiarchaeum*.

For some filters with a 0.1 µm and 0.2 µm pore size, the number of Huberarchaeota per Altiarchaeota increase, indicating that *Ca.* Huberiarchaeum has a small cell size [10] and thus passes through the larger filters while *Ca.* Altiarchaeum does not.

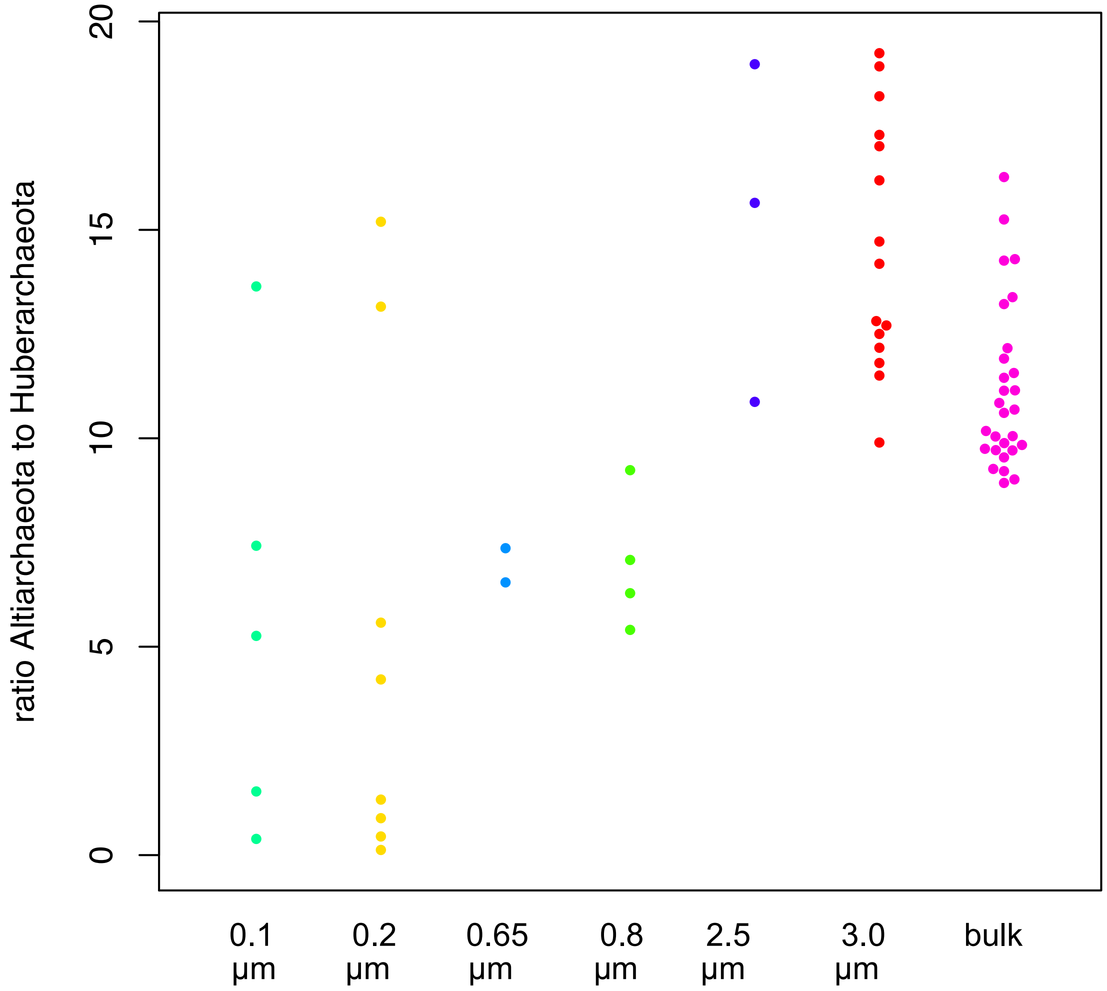

Fig. S4 | Counts of FISH signals showing associations of Altiarchaeota and Huberarchaeota as well as single Altiarchaeota and single Huberarchaeota cells. Counts were summarized from three different sample preparations across 46 cell-positive fields of view. Example images can be found in main *Fig 1C*.

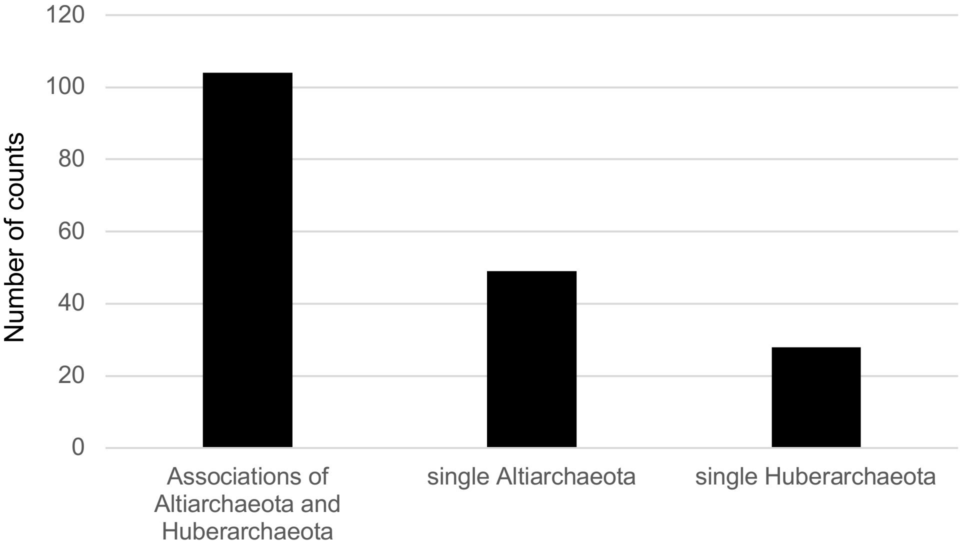

Fig. S5 | Detailed metabolic reactions of predicted enzymes from Supplementary Table 1 and 2. Summary is provided in main *Fig. 2*.

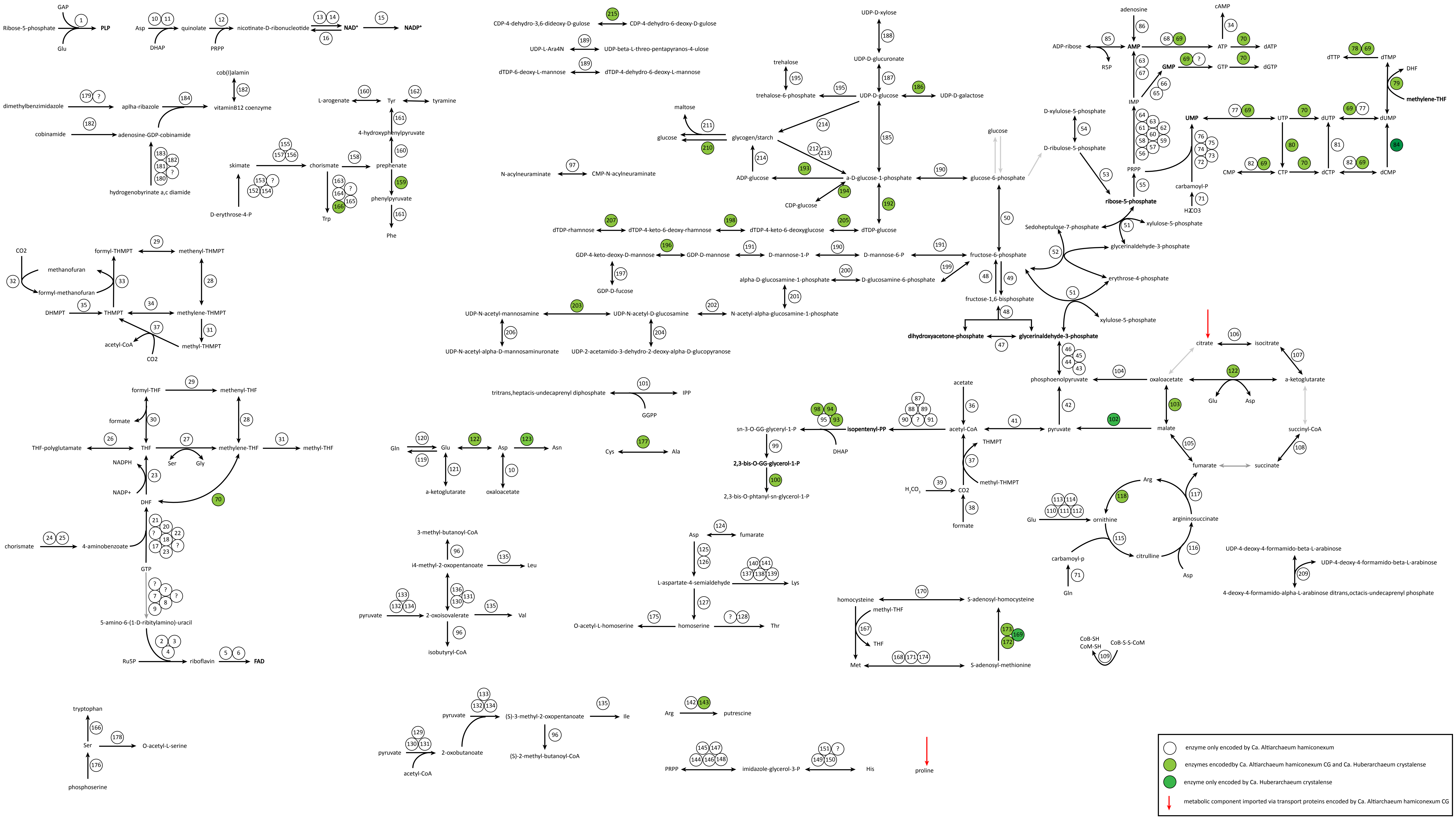
Ribose-5-phosphate
GAP
Glu
PLP
Asp
DHAP
quinolate
PRPP
nicotinate-D-ribonucleotide
NAD+
NADP+
cob(I)alamin
dimethylbenzimidazole
aplha-ribazole
vitaminB12 coenzyme
cobinamide
adenosine-GDP-cobinamide
hydrogenobyrinate a,c diamide
L-arogenate
Tyr
tyramine
4-hydroxyphenylpyruvate
skimate
chorismate
prephenate
phenylpyruvate
D-erythrose-4-P
Trp
Phe
CO2
methanofuran
formyl-methanofuran
formyl-THMPT
methenyl-THMPT
DHMPT
THMPT
methylene-THMPT
methyl-THMPT
acetyl-CoA
formyl-THF
methenyl-THF
formate
THF-polyglutamate
THF
methylene-THF
methyl-THF
Ser
Gly
NADPH
NADP+
DHF
chorismate
4-aminobenzoate
GTP
5-amino-6-(1-D-ribitylamino)-uracil
Ru5P
riboflavin
FAD
tryptophan
O-acetyl-L-serine
phosphoserine
CDP-4-dehydro-3,6-dideoxy-D-gulose
CDP-4-dehydro-6-deoxy-D-gulose
UDP-L-Ara4N
UDP-beta-L-threo-pentapyranos-4-ulose
dTDP-6-deoxy-L-mannose
dTDP-4-dehydro-6-deoxy-L-mannose
N-acylneuraminate
CMP-N-acylneuraminate
UDP-D-xylose
UDP-D-glucuronate
trehalose
trehalose-6-phosphate
UDP-D-glucose
UDP-D-galactose
maltose
glucose
glycogen/starch
ADP-glucose
a-D-glucose-1-phosphate
CDP-glucose
glucose-6-phosphate
dTDP-rhamnose
dTDP-4-keto-6-deoxy-rhamnose
dTDP-4-keto-6-deoxyglucose
dTDP-glucose
GDP-4-keto-deoxy-D-mannose
GDP-D-mannose
D-mannose-1-P
D-mannose-6-P
fructose-6-phosphate
GDP-D-fucose
alpha-D-glucosamine-1-phosphate
D-glucosamine-6-phosphate
fructose-1,6-bisphosphate
UDP-N-acetyl-mannosamine
UDP-N-acetyl-D-glucosamine
N-acetyl-alpha-glucosamine-1-phosphate
UDP-N-acetyl-alpha-D-mannosaminuronate
UDP-2-acetamido-3-dehydro-2-deoxy-alpha-D-glucopyranose
dihydroxyacetone-phosphate
glycerinaldehyde-3-phosphate
tritrans,heptacis-undecaprenyl diphosphate
IPP
GGPP
Cys
Ala
Gln
Glu
Asp
Asn
a-ketoglutarate
oxaloacetate
3-methyl-butanoyl-CoA
i4-methyl-2-oxopentanoate
Leu
pyruvate
2-oxoisovalerate
Val
isobutyryl-CoA
pyruvate
(S)-3-methyl-2-oxopentanoate
Ile
(S)-2-methyl-butanoyl-CoA
2-oxobutanoate
acetyl-CoA
sn-3-O-GG-glyceryl-1-P
isopentenyl-PP
DHAP
2,3-bis-O-GG-glycerol-1-P
2,3-bis-O-phtanyl-sn-glycerol-1-P
Asp
fumarate
L-aspartate-4-semialdehyde
Lys
O-acetyl-L-homoserine
homoserine
Thr
Arg
putrescine
PRPP
imidazole-glycerol-3-P
His
proline
acetate
acetyl-CoA
pyruvate
THMPT
methyl-THMPT
H2CO3
CO2
formate
homocysteine
S-adenosyl-homocysteine
methyl-THF
THF
Met
S-adenosyl-methionine
adenosine
ADP-ribose
R5P
AMP
ATP
dATP
cAMP
GMP
GTP
dGTP
IMP
D-xylulose-5-phosphate
D-ribulose-5-phosphate
PRPP
ribose-5-phosphate
UMP
UTP
dUTP
dUMP
dTTP
dTMP
DHF
methylene-THF
CMP
CTP
dCTP
dCMP
carbamoyl-P
H2CO3
Sedoheptulose-7-phosphate
xylulose-5-phosphate
glycerinaldehyde-3-phosphate
erythrose-4-phosphate
xylulose-5-phosphate
glucose
phosphoenolpyruvate
citrate
isocitrate
oxaloacetate
Glu
Asp
a-ketoglutarate
malate
succinyl-CoA
fumarate
succinate
Arg
Glu
ornithine
argininosuccinate
citrulline
carbamoyl-p
Gln
Asp
UDP-4-deoxy-4-formamido-beta-L-arabinose
UDP-4-deoxy-4-formamido-beta-L-arabinose
4-deoxy-4-formamido-alpha-L-arabinose ditrans,octacis-undecaprenyl phosphate
CoB-SH
CoM-SH
CoB-S-S-CoM
○ enzyme only encoded by Ca. Altiarchaeum hamiconexum
● enzymes encodedby Ca. Altiarchaeum hamiconexum CG and Ca. Huberarchaeum crystalense
● enzyme only encoded by Ca. Huberarchaeum crystalense
↓ metabolic component imported via transport proteins encoded by Ca. Altiarchaeum hamiconexum CG

4. Description of Supplementary Data

Supplementary Data file 1.
Table summarizing the genomes used for the maximum likelihood and Bayesian phylogenetic analyses. Includes the NCBI assembly accession ID, taxonomic affiliation as well as CheckM results and number of marker genes identified using phylosift.

Supplementary Data file 2
Raw tree file of the maximum likelihood tree displayed in *Fig. 1A*. It includes 186 taxa and was inferred based on an alignment of 34 marker genes with 4224 positions in IQ-tree under the LG+C60+F+R model. Bootstrap support was inferred using an SH-like approximate likelihood ratio test and ultrafast bootstrap support values. Scale bar indicates the average number of substitutions per site.

Supplementary Data file 3
Raw tree file of the maximum likelihood analysis based on the recoded alignment used in the analysis shown in *Fig. 1A*. It includes 186 taxa and was inferred based on a SR4-recoded alignment of 34 marker genes with 4224 positions in IQ-tree under the LG+C60+F+R model. Bootstrap support was inferred using an SH-like approximate likelihood ratio test and ultrafast bootstrap support values. Scale bar indicates the average number of substitutions per site.

Supplementary Data file 4
Raw tree of the Bayesian phylogenetic analysis based on the concatenated alignment of the 34 marker genes with 4288 sites using 124 representative archaeal taxa. The tree represents a consensus generated from 2 chains, sampling every fifth generation (maxdif: 0.14). Values at branches refer to posterior probability support.

Supplementary Data file 5
Raw tree of the Bayesian phylogenetic analysis based on the recoded concatenated alignment of the 34 marker genes with 4288 sites using 124 representative archaeal taxa. The tree represents a consensus generated from 2 chains, sampling every fifth generation (maxdif: 0.14). Values at branches refer to posterior probability support.

4. References

1. Darling AE, Jospin G, Lowe E, Matsen IV FA, Bik HM, Eisen JA. PhyloSift: phylogenetic analysis of genomes and metagenomes. *PeerJ* 2014; **2**: e243.
2. Becker EA, Seitzer PM, Tritt A, Larsen D, Krusor M, Yao AI, et al. Phylogenetically driven sequencing of extremely halophilic archaea reveals strategies for static and dynamic osmo-response. *PLoS Genet* 2014; **10**: e1004784.
3. Katoh K, Misawa K, Kuma K, Miyata T. MAFFT: a novel method for rapid multiple sequence alignment based on fast Fourier transform. *Nucleic Acids Res* 2002; **30**: 3059–3066.
4. Probst AJ, Weinmaier T, Raymann K, Perras A, Emerson JB, Rattei T, et al. Biology of a widespread uncultivated archaeon that contributes to carbon fixation in the subsurface. *Nat Commun* 2014; **5**: 5497.
5. Susko E, Roger AJ. On reduced amino acid alphabets for phylogenetic inference. *Mol Biol Evol* 2007; **24**: 2139–2150.
6. Zaremba-Niedzwiedzka K, Caceres EF, Saw JH, Bäckström D, Juzokaite L, Vancaester E, et al. Asgard archaea illuminate the origin of eukaryotic cellular complexity. *Nature* 2017; **541**: 353–358.
7. Guindon S, Dufayard J-F, Lefort V, Anisimova M, Hordijk W, Gascuel O. New algorithms and methods to estimate maximum-likelihood phylogenies: assessing the performance of PhyML 3.0. *Syst Biol* 2010; **59**: 307–321.
8. Minh BQ, Nguyen MAT, von Haeseler A. Ultrafast approximation for phylogenetic bootstrap. *Mol Biol Evol* 2013; **30**: 1188–1195.
9. Lartillot N, Philippe H. A Bayesian mixture model for across-site heterogeneities in the amino-acid replacement process. *Mol Biol Evol* 2004; **21**: 1095–1109.
10. Probst AJ, Ladd B, Jarett JK, Geller-McGrath DE, Sieber CMK, Emerson JB, et al. Differential depth distribution of microbial function and putative symbionts through sediment-hosted aquifers in the deep terrestrial subsurface. *Nat Microbiol* 2018; **3**: 328–336.
11. Edgar RC. Search and clustering orders of magnitude faster than BLAST. *Bioinformatics* 2010; **26**: 2460–2461.
12. Vallenet D, Labarre L, Rouy Z, Barbe V, Bocs S, Cruveiller S, et al. MaGe: a microbial genome annotation system supported by synteny results. *Nucleic Acids Res* 2006; **34**: 53–65.
13. Kanehisa M, Sato Y, Kawashima M, Furumichi M, Tanabe M. KEGG as a reference resource for gene and protein annotation. *Nucleic Acids Res* 2016; **44**: D457–D462.
14. Probst AJ, Castelle CJ, Singh A, Brown CT, Anantharaman K, Sharon I, et al. Genomic resolution of a cold subsurface aquifer community provides metabolic insights for novel microbes adapted to high CO2 concentrations. *Environ Microbiol* 2017; **19**: 459–474.
15. Emerson JB, Thomas BC, Alvarez W, Banfield JF. Metagenomic analysis of a high carbon dioxide subsurface microbial community populated by chemolithoautotrophs and bacteria and archaea from candidate phyla. *Environ Microbiol* 2016; **18**: 1686–1703.
16. Brown CT, Olm MR, Thomas BC, Banfield JF. Measurement of bacterial replication rates in microbial communities. *Nat Biotechnol* 2016.
17. R Core T. R: A language and environment for statistical computing. *Online http://www.r-proj.org* 2016.

18. Langmead B, Salzberg SL. Fast gapped-read alignment with Bowtie 2. *Nat Methods* 2012; **9**: 357–359.
19. propr: An R-package for Identifying Proportionally Abundant Features Using Compositional Data Analysis. *Sci Rep* 2017; **7**:16252.
20. Lovell D, Pawlowsky-Glahn V, Egozcue JJ, Marguerat S, Bähler J. Proportionality: a valid alternative to correlation for relative data. *PLoS Comput Biol* 2015; **11**: e1004075.
21. Csardi G, Nepusz T. The igraph software package for complex network research. *InterJournal Complex Syst* 2006; 1695.
22. Ludwig W, Strunk O, Westram R, Richter L, Meier H, Yadhukumar, et al. ARB: a software environment for sequence data. *Nucleic Acids Res* 2004; **32**: 1363–1371.
23. Rudolph C, Wanner G, Huber R. Natural communities of novel archaea and bacteria growing in cold sulfurous springs with a string-of-pearls-like morphology. *Appl Environ Microbiol* 2001; **67**: 2336–2344.
24. Yilmaz LS, Parnerkar S, Noguera DR. mathFISH, a web tool that uses thermodynamics-based mathematical models for in silico evaluation of oligonucleotide probes for fluorescence in situ hybridization. *Appl Environ Microbiol* 2011; **77**: 1118–1122.